THE SEISMOLOGICAL SOCIETY OF AMERICA
400 Evelyn Ave., Suite 201
Albany, CA 94706-1375
(510) 525-5474; FAX (510) 525-7204
www.seismosoc.org

Bulletin of the Seismological Society of America, 89, 6, pp. 1543–1557, December 1999

The Effect of Local Wind on Seismic Noise near 1 Hz at the MELT Site and in Iceland

by William S. D. Wilcock, Spahr C. Webb, and Ingi Th. Bjarnason

Abstract The mantle electromagnetic and tomography (MELT) experiment on the east Pacific rise near 17°S was the first large teleseismic experiment on a midocean ridge. During the six-month deployment, no compressional arrivals were well recorded above 0.5 Hz. In comparison, the ICEMELT experiment in Iceland recorded compressional arrivals at 1–2 Hz from about 2 earthquakes per month. We compare noise spectra from the two experiments and show that this difference in detection is at least in part a result of noise. Near 1 Hz, seismic noise in the oceans is produced locally by wind-generated waves. At both experiment sites, 1-Hz noise levels are well correlated with local sea-surface-wind speeds derived from satellite observations. For a given wind speed, 1-Hz noise levels are about 10–20 dB lower in Iceland. At the MELT site, cross-correlations of wind speed with the logarithm of noise in a narrow-frequency band yield correlation coefficients exceeding 0.7 at frequencies between 0.4 Hz and 2 Hz. Noise levels at 1 Hz increase with wind by 1.3–1.4 dB per m/sec for wind speeds less than 10 m/sec. For the ICEMELT experiment, high correlation coefficients extend to markedly higher frequencies for coastal stations, and there is a 10-dB drop in 1-Hz noise levels 100-km inland. Noise levels increase by about 0.8 dB per m/sec. The strong correlation between wind speed and 1-Hz seismic noise provides justification for using satellite wind speed data to search for locations on the global spreading system where there is a better probability of recording high-frequency arrivals. The calmest sites are found on the northern east Pacific rise, near the equator in all oceans, and near 34° N and 22° S on the mid-Atlantic ridge.

Introduction

Autonomous ocean bottom seismographs (OBSs) have been in widespread use for over 25 years. For most of this period, experiments were confined largely to short refraction and microearthquake deployments because of the limited endurance of the instruments. In recent years, improvements in low-power electronics and clock technology have facilitated the construction of OBSs that can be deployed for periods of one year. Broadband pressure sensors have been available for some time (Cox *et al.,* 1984) and with careful electronic design, it is now possible to record ground motion with conventional 1-Hz geophones at periods longer than 50 sec. These technological advances are expanding the variety and characteristics of marine seismology experiments. Passive microearthquake studies are increasing in length, and it is now feasible to conduct regional scale marine experiments to record teleseismic arrivals. Autonomous OBSs may also play a role in plans to fill in the oceanic gaps in global seismic networks (Purdy and Dziewonski, 1988; Orcutt and Purdy, 1995).

As for all seismic observations, the ability of OBSs to record teleseismic arrivals is dependent not only on signal strength and instrument characteristics, but also on noise levels. In the microseismic band that extends from 0.1 to about 5 Hz, wind-driven gravity waves on the sea surface are the dominant source of seismic noise, and the seafloor is often a noisy environment (Webb, 1998). Previous experience (Blackman *et al.,* 1995) and quantitative considerations (Webb, 1998) suggest that compressional arrivals near 1 Hz will only be well recorded for very large earthquakes or during calm periods. However, there are still relatively few recordings of teleseisms in the deep ocean, and most were not made on well-calibrated OBSs. Only a few deep-water experiments have simultaneously monitored microseismic noise and surface wind and wave conditions (Adair *et al.,* 1984; Babcock *et al.,* 1994; Dorman *et al.,* 1993; Lewis and Dorman, 1992; McCreery *et al.,* 1993). None of the data have been adequate to assess the probability of recording high-frequency teleseisms.

The Mantle Electromagnetic and Tomography (MELT) experiment (Forsyth *et al.,* 1998) near 17°S on the east Pa-

cific rise (EPR) was the first large-scale long-term deployment of OBSs on a midocean ridge with the primary objective of recording teleseismic arrivals. The experiment was designed to distinguish between competing models of upper mantle flow and melt generation beneath midocean ridges and consisted of 51 OBSs deployed for 6 months in two linear arrays across the ridge axis (Fig. 1). The data collected facilitated a variety of complementary studies involving teleseismic body waves, surface waves, and local data (Forsyth *et al.,* 1998) but no high-frequency teleseismic arrivals were recorded, a disappointing although not entirely unexpected result. While there was a reasonable distribution of earthquakes during the deployment (Forsyth *et al.,* 1998), no clear teleseismic compressional arrivals were recorded above about 0.5 Hz. Two-dimensional tomographic images of across-axis variations in mantle *P*-wave structure (Toomey *et al.,* 1998) were obtained with picks made from 12 earthquakes in the 0.15–0.5 Hz band.

In contrast to MELT, the ICEMELT experiment (Bjarnason *et al.,* 1996), which deployed up to 14 broadband seismometers throughout Iceland (Fig. 1), recorded about 50 earthquakes with a good signal-to-noise ratio above 1 Hz over a 26-month period. Travel-time picks from 86 earthquakes obtained at frequencies between about 0.5 and 2 Hz were inverted for a three-dimensional model of *P*-wave-velocity structure in the Iceland mantle plume (Wolfe *et al.,* 1997). Since travel-time picks obtained from high-frequency arrivals have smaller uncertainties and the optimal resolution

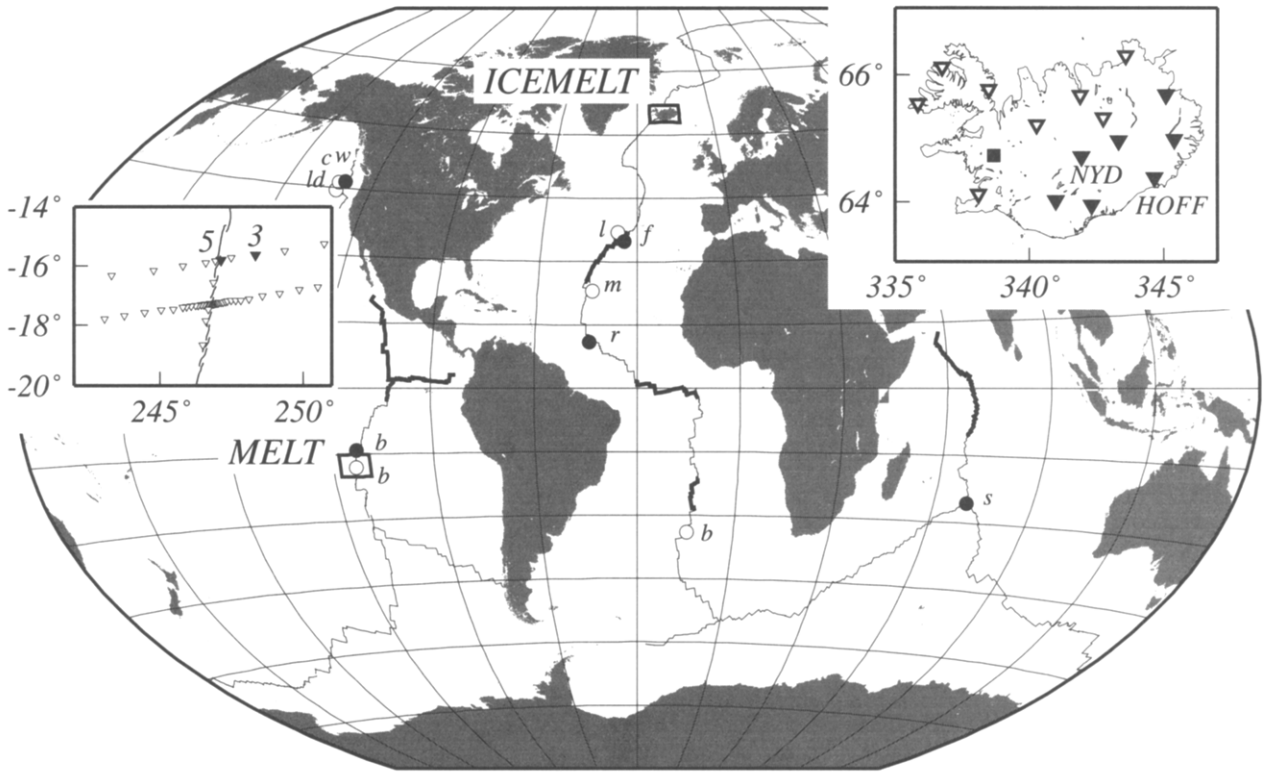

Figure 1. Map showing the global network of major midocean ridges (Coffin *et al.,* 1998). Bold lines show spreading centers where the analysis of a global model that incorporates satellite-derived wind speeds suggests that there is a higher probability of recording high-frequency teleseismic *P* waves (see text). Also shown are sites on the midocean ridge network where deployments prior to the MELT experiment have recorded teleseismic compressional arrivals near 1 Hz (filled circles) and only below 0.2 Hz (open circles). Labels refer to the source of the observations as follows: b, Blackman *et al.* (1995); c, Crawford *et al.* (1993); f, Forsyth (1996) and Blackman *et al.* (1995); l, Levchenko *et al.* (1994); ld, Lewis and Dorman (1992); m, Montagner *et al.* (1994); r, Rowlett and Forsyth (1979); and w, Webb (1998). Two boxes delineate the areas of inset maps, which show the configuration of the MELT and ICEMELT experiments. For the MELT experiment, the inset map show the spreading center (solid lines) and stations that returned data (triangles). The two stations (sites 3 and 5) used extensively in this study are shown are labeled and are shown as solid symbols. For the ICEMELT experiment, the network comprised 14 temporary installations (triangles) and Global Seismic Network (GSN) station BORG (square). The stations used for this study are shown as solid symbols and include stations NYD near the center of the island and HOFF near the southeast coast.

of the tomographic images is limited by the seismic wavelength, it would clearly be advantageous to locate future body wave experiments on midocean ridge segments where the probability of recording clear high-frequency arrivals can be maximized.

In this article, we compare noise levels from the MELT and ICEMELT experiment. The absence of high-frequency compressional arrivals in the MELT data can be attributed, at least in part, to higher noise levels in the region. The noise spectra are consistent with the current understanding of microseismic noise generation and propagation. We make use of a global wind data set derived from conventional and satellite measurements to explore the relationships between local wind and noise at the two sites. Near 1 Hz, the noise is well correlated with local wind, particularly at the MELT site. We use the wind data set to search for locations on the global midocean ridge system where there is a relatively high probability of recording high-frequency body waves.

Noise Observed in the MELT and ICEMELT Experiments

Figure 2 shows compressional arrivals recorded during the MELT and ICEMELT experiments for two similar earthquakes. The MELT example is one of the best recorded short-period teleseisms in that experiment. At 0.03–0.1 Hz, both events are recorded with a large signal-to-noise ratio, although noise levels are lower for the ICEMELT example. Between 0.1 and 1 Hz, signal-to-noise ratios are mediocre for both events. The ICEMELT event is slightly better recorded at 0.1–0.3 Hz, while the signal-to-noise ratio is better for the MELT event at 0.3–1 Hz, particularly on the vertical seismometer. The most striking difference between the recordings occurs at 1–3 Hz. Here root mean squared noise levels on the normalized seismograms are about 8 times higher for MELT, and the arrival is barely visible. Although differences in the source and path characteristics may affect the amplitude of teleseismic arrivals significantly, it is clear from a comparison of noise power spectra obtained just prior to the example earthquakes (Fig. 3) that differing noise levels contribute substantially to the large difference in signal to noise near 1 Hz. Between 0.5 and 2 Hz, noise levels at the MELT site are about 20 dB higher.

The processes responsible for generating microseismic noise are well understood, and we have a reasonable knowledge of the gross variations in noise spectra that might be expected between different regions of the oceans (Webb, 1998). Microseisms are a consequence of a nonlinear interaction between surface gravity waves traveling in opposite or nearly opposite directions, which results in noise at twice the wave frequency (the frequency doubling effect) (Kibblewhite and Wu, 1991, 1996; Orcutt *et al.,* 1993). The formation of ocean waves is dependent on the wind speed, duration, and fetch. At short periods, the sea surface can respond quickly to local winds, while at longer periods a substantial fetch and duration are required for the seas to build (Massel, 1995). For fully developed seas (Fig. 4), the dominant wave period and amplitude increases with wind speed. Waves with periods much shorter than the dominant period reach saturation amplitudes that decrease sharply with increasing frequency. Since microseisms require waves traveling in opposite directions, their generation will be particularly efficient when the waves from two sources interact or when winds shift. However, even under a steady unidirectional wind, the wave spectrum will have a significant components traveling in opposing directions (Massel, 1995). In contrast, the swell from a single distant source is unidirectional and is not expected to be a significant source (Webb, 1998). Microseisms tend to form in or near the same regions where the waves are produced.

Ocean waves with periods above 25 sec are extremely rare, and 10–15 sec waves are commonly produced by large storms. As a result, seismic noise increases sharply from about 0.1 Hz to a maximum value typically at 0.15–0.2 Hz. Microseismic noise propagates away from source regions primarily as Rayleigh waves. At lower frequencies, these attenuate slowly, and the 7-sec microseismic peak is a prominent feature of noise spectra even in the center of continents. As the frequency increases, microseisms attenuate more rapidly with distance. Near 1 Hz, seafloor noise is primarily dependent on local weather conditions (Dorman *et al.,* 1993; Webb, 1992, 1998; Babcock *et al.,* 1994; Bromirski and Duennebier, 1998). In many regions, the ocean wind speeds are sufficient to produce saturated wave amplitudes at frequencies above ~1 Hz (Webb, 1992), and the resulting universal noise spectrum is termed the HOLU spectrum (McCreery *et al.,* 1993). Since saturated wave amplitudes decrease rapidly with frequency (Fig. 4), the saturated seismic noise levels also decline.

The example ICEMELT earthquake shown in Figure 2 occurred during the summer when large regions of the North Atlantic are often calm. As a result, low-frequency microseismic noise levels are low, and the microseismic peak occurs at 0.2–0.3 Hz (Fig. 3). In contrast, the Pacific Ocean is sufficiently large enough that storms at high southern latitudes produce a fairly consistent microseismic peak near 0.15 Hz. The MELT site lies in the tropics and is fairly distant from the largest storms, so peak microseismic noise levels are not particularly high. In the winter, there are many big storms near Iceland, and the microseismic peak is typically about 30 dB higher than in the summer months and about 20 dB higher than the MELT site (Fig. 3). The peak winter noise level of $\sim 10^9$ m^2 s^{-4} Hz^{-1} is in reasonable agreement with measurements on the North Atlantic seafloor (Babcock *et al.,* 1994).

The EPR at 17°S sits in the southeasterly trades. These winds are strong enough to generate substantial microseismic noise above 0.5 Hz, which makes the MELT site a noisy environment near 1 Hz. In Iceland, the 1-Hz noise levels are substantially lower and not as strongly dependent on the season as the microseismic peak. The ICEMELT examples (Fig. 3) show that noise levels between 0.5 and 1 Hz are

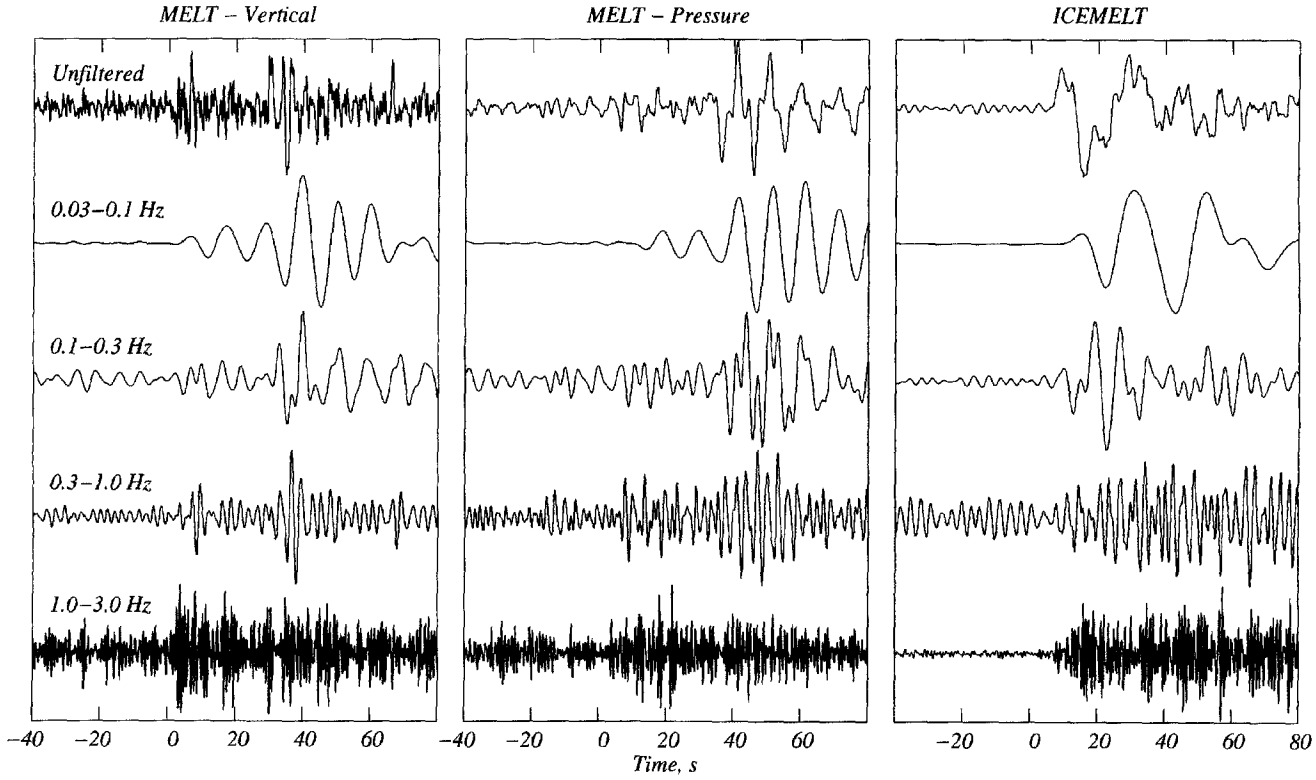

Figure 2. Examples of P waves recorded during the MELT and ICEMELT experiments. The left hand panel shows the vertical channel at MELT site 5 for an earthquake that occurred south of the Fiji Islands at 00:30 GMT on April 16, 1996 ($\Delta = 61°$, $M = 7.1$, and $Z = 111$ km). The center panel shows the pressure record at a nearby site for the same earthquake. The right hand panel shows the vertical channel at ICEMELT station NYD for an earthquake near the Andreanof Islands at 15:24 GMT on June 10, 1996 ($\Delta = 63°$, $M_s = 7.1$, $Z = 26$ km). Each panel shows the unfiltered record and four traces that have been filtered into the pass bands of 0.03–0.1 Hz, 0.1–0.3 Hz, 0.3–1 Hz, and 1–3 Hz. The instrument response has been deconvolved from each filtered trace and a fourth order minimum phase bandpass butterworth filter applied. The traces are plotted with equal maximum amplitude.

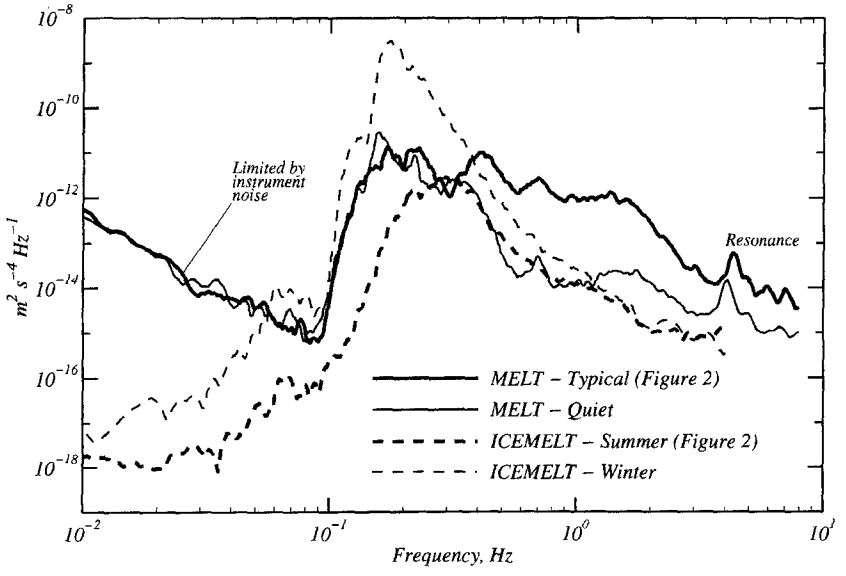

Figure 3. Smoothed noise power spectra for the vertical acceleration at MELT site 5 (solid) and ICEMELT station NYD (dashed). The bold lines show noise spectra recorded prior to the earthquakes shown in Figure 2. A thin solid line shows noise levels during a short period of quiet conditions early in the MELT experiment. The thin dashed line shows typical noise levels recorded on Iceland during the winter (the bold dashed line is typical of summer). Note that for the MELT experiment, there is an instrument or ground resonance near 4 Hz and the noise levels are instrumental below 0.1 Hz.

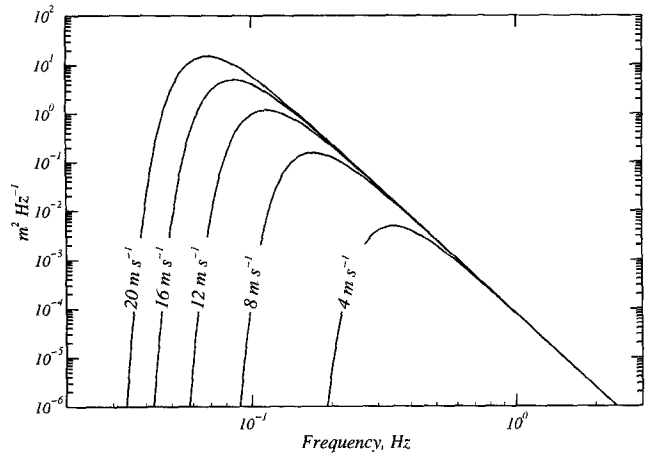

Figure 4. The Pierson and Moskowitz (1964) model for the wave height power spectrum in a fully developed sea for wind speeds of 4, 8, 12, 16, and 20 m/sec.

only about 5 dB lower in summer and are virtually unchanged above 1 Hz. Figure 3 also shows a noise spectrum recorded at the MELT site during a short period of unusual quiet. The microseismic peak is not shifted in frequency or amplitude, but the 0.5–1 Hz noise levels are similar to those in Iceland. Unfortunately, no significant teleseisms occurred during such intervals in MELT.

Below 0.1 Hz the noise spectra for MELT and Iceland differ for several reasons. Ambient noise levels are sufficiently low at longer periods, so instrumental noise dominates the MELT seismometer below 0.1 Hz and the pressure sensor between 0.03 and 0.1 Hz even though the noise characteristics of the instrument are quite good. Below 0.03 Hz, surface gravity waves (infragravity waves) reach the seafloor and pressure noise levels on the seafloor are consequently much higher than on land (Webb *et al.*, 1991). During winter, elevated noise levels at 0.05–0.1 Hz are visible in spectra for Iceland. This is the single-frequency microseismic noise that is produced by the direct interaction of waves with the seafloor in shallow water (Hasselmann, 1963).

Comparisons with Local Wind Speeds

A Satellite Derived Wind Speed Data Set

On land, there are many stations reporting winds, but conventional measurements in the oceans are limited to islands and a relatively small number of unevenly distributed buoys and ships. Fortunately it is also possible to determine wind speeds by remote sensing. Both passive and active microwave measurements can be used to sense the effects of wind-generated capillary waves. From a meteorological standpoint, active measurements are advantageous because they determine the wind direction in addition to the speed. They are also technologically more challenging, and only a limited amount of data presently exists. Passive measurements have been obtained almost continuously for the past 20 years. Since 1987, data has been available from the Special Sensor Microwave Imager (SSM/I) flown by the Defense Meteorological Satellite Program (DMSP). The SSM/I (Hollinger *et al.*, 1987) has 7 radiometers that measure ocean brightness at 4 frequencies; this data can be used to estimate surface wind speed, columnar water vapor, and columnar cloud liquid (Wentz, 1997). Each DSMP satellite provides complete global coverage every day, although wind speed estimates are not available when it rains. At least two satellites have been in operation since 1991. The latest algorithm available to reduce the data provides sea-surface wind measurements with an uncertainty of 1 m/sec and a spatial resolution of 50 km (Wentz, 1997).

In order to get a continuous and evenly spaced time series of wind speeds over both the ocean surface and land, we use a global data set prepared by combining conventional wind analyses with the SSM/I data (Atlas *et al.*, 1996). The European Center for Medium-Range Weather Forecasts (ECMWF) provides atmospheric models derived by a consistent assimilation of a wide variety of data (not including SSM/I) into a sophisticated forecasting algorithm (Trenberth, 1992). Atlas *et al.* (1996) use a variational method to combine the ECMWF analyses with the SSM/I data and conventional ocean wind velocity measurements. They solve for perturbations to the ECMWF surface winds by minimizing an objective function comprising data misfits and *a priori* constraints on the smoothness, divergence, and vorticity of the perturbations. The model is available on six hourly intervals with grid points spaced 2 degrees apart in latitude and 2.5 degrees in longitude. Comparisons with Tropical Atmosphere Ocean (TAO) buoys near the equator that were not used in the analysis reveal a root mean square (rms) wind speed error of 1.4 m/sec and a bias of only 0.2 m/sec. The rms misfit for all buoys is 2.0 m/sec with a bias of 0.3 m/sec.

The MELT Site

To investigate temporal variations in noise levels at the MELT site, we calculated spectra at 1-hour intervals for the entire duration of the experiment. To minimize the effects of teleseisms and local earthquakes, we discarded spectra during intervals in which the average spectral amplitude in either the 0.03- to 1-Hz or 2- to 5-Hz band increased by 10 dB above the previous spectrum. Comparisons with an earthquake catalog and inspection of seismograms shows that this process successfully eliminates most spectra that contain significant earthquakes or other short-term transient energy.

Figure 5 compares a time series of satellite derived wind speeds with logarithmic noise levels at two MELT sites near 0.3, 1, and 4 Hz. Each time series has been smoothed with a 3-day running mean. At 0.3 Hz, seismic noise and local wind are not well correlated. For instance, the period of low wind speed late in 1995 coincides with high noise at 0.3 Hz, even though the wind speed is generally low everywhere within a 1000 km of the MELT site. In contrast, there is a remarkably good correlation between noise and wind at 1

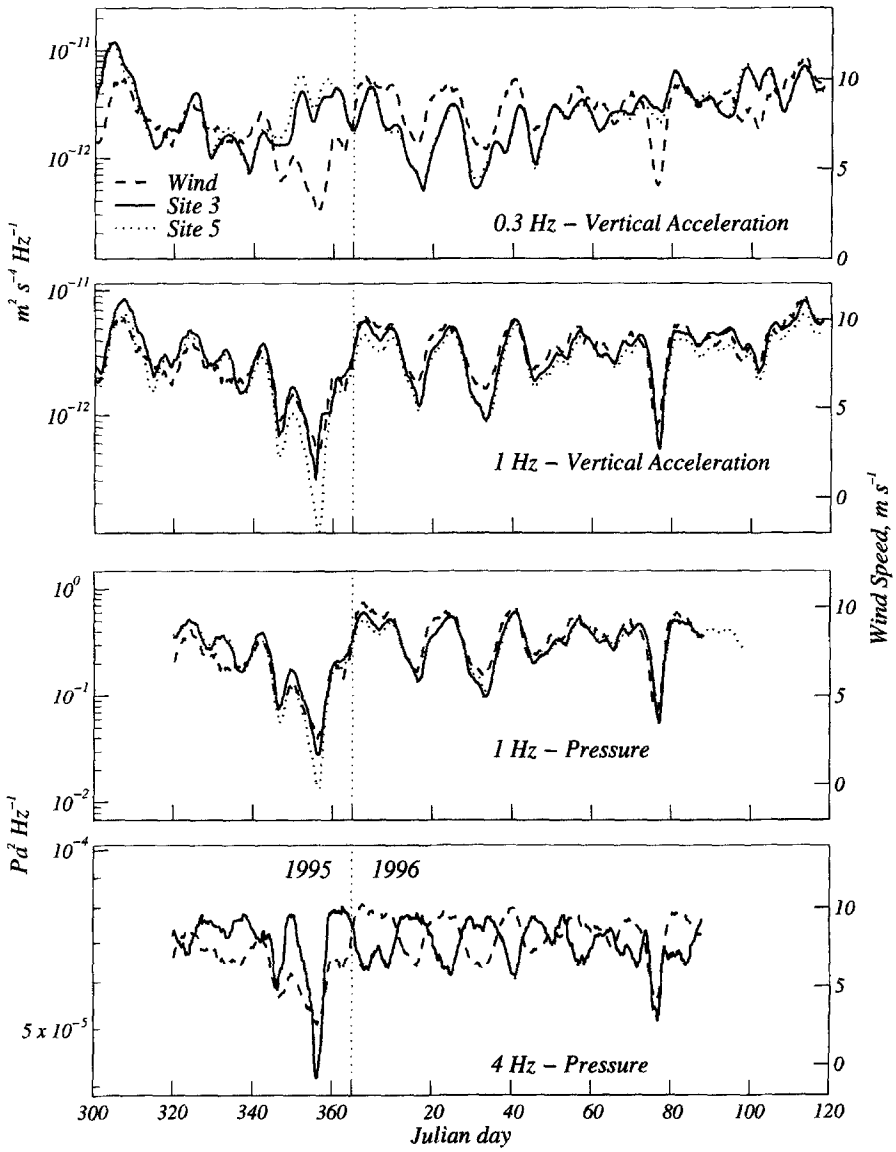

Figure 5. Time series comparing noise levels on a logarithmic scale with wind speed in the MELT experiment. Noise levels at site 3 (solid) and site 5 (dotted) have been obtained by averaging power spectral values in 0.3 octave bands centered on 0.3 and 1 Hz for vertical acceleration and 1 and 4 Hz for pressure. The wind speed (dotted) is from a global data set derived from satellite data (Atlas *et al.*, 1996). Time series have been smoothed with a 3-day running mean and the scaling has been chosen so as to minimize the misfit between the noise and wind data.

Hz. For most of the experiment, wind speeds remain above 5 m/sec and average over 8 m/sec. There are two short intervals where the smoothed wind speeds drop below 3 and 4 m/sec, and these are associated with drops in noise levels of up to 25 dB and 15 dB, respectively. Noise levels at 4 Hz also decline during these two intervals of relative calm, but for the rest of the experiment the noise and wind are clearly anticorrelated. A similar phenomenon has also been observed by McCreery *et al.* (1993) near Wake Island. They argue that strong winds may blow the tops off short-period waves and beat them down with spray.

We computed cross-correlation coefficients between wind speed and logarithmic noise at a variety of frequencies. We used unsmoothed data and searched for the maximum correlation coefficient with an absolute lag of up to 4 days. Between 0.4 and 2 Hz the correlation coefficient exceeds 0.7 (Figure 6) and reaches a maximum of 0.8 near 1 Hz. Cross-correlations of the wind at the MELT site with the regional wind field fall below 0.8 at ranges of about 500 km and 300 km in east–west and north–south directions, respectively. Noise near 1 Hz is clearly generated within no more than a few hundred kilometers of the experiment site. At frequen-

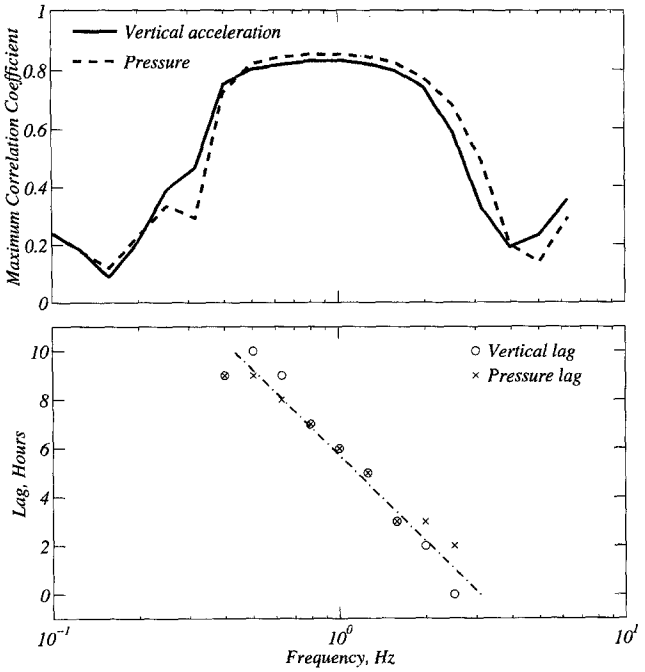

Figure 6. Results of cross-correlating noise levels in 0.3 octave bands with wind speed at MELT site 3. The upper panel shows the maximum correlation coefficient as a function of frequency for vertical acceleration (solid) and pressure (dashed) noise. The lower panel shows noise lag for maximum correlation coefficients exceeding 0.5 for vertical acceleration (circles) and pressure (crosses). The lags are fit well by a relationship of the form $l = 5.7 - 11.6 \log_{10} f$ where l is the lag in hours and f the frequency (dot-dashed line).

cies where the wind and noise time series are well correlated, the noise lags the wind. The lag time decreases linearly with the logarithm of frequency from about 10 hours at 0.5 Hz to 2 hours at 2 Hz (Fig. 6). This is a reflection of the time required for the sea to build and decay.

Scatter plots of vertical acceleration and pressure noise levels against wind speed (Fig. 7) also show little correlation between wind and seismic noise near 0.3 Hz, while at frequencies of 0.5 Hz and above, noise increases with wind speed. At 2 and 4 Hz, the noise clearly reaches saturation levels. Between 1 and 4 Hz, saturation noise levels decrease by about 20 dB/octave, a result that is in reasonable agreement with the value of −23 dB/octave reported near Wake Island (McCreery *et al.,* 1993). At 0.5 and 1.0 Hz, least-squares straight-line fits to the data show that noise levels increase with wind speed at about 1.3–1.4 dB per m/sec, and at 2 Hz the slope below the saturation threshold of about 7 m/sec is closer to 2 dB per m/sec. These results are also generally consistent with the results of McCreery *et al.* (1993).

Although there is substantial scatter in the data, it is clear that noise levels saturate at wind speeds that are much higher than those required to produce saturated wave amplitudes in the model by Pierson and Moskowitz (1964) (Fig. 4). For instance, at 0.5 Hz the Pierson and Moskowitz (1964) wave power spectrum reaches 90% of the saturation value at 4.3 m/sec, but 1-Hz noise levels at the MELT site do not appear to saturate until around 10 m/sec. We suspect that this discrepancy is a consequence of systematic variations in the directional spectra of the waves. Microseism generation requires waves traveling in nearly opposing directions and will be enhanced by a broad directional spectrum. It is well known that the directional spectrum of short-period waves broadens as the wind speed increases (Massel, 1995).

In Figure 7 we show noise predictions for an infinite-depth ocean model obtained using the method outlined in Webb (1992). The noise levels are based on the wave height spectrum by Pierson and Moskowitz (1964). We assume the microseisms are generated by waves with nearly opposite wave numbers so that the difference in wave numbers corresponds to an acoustic wave in the ocean (Kibblewhite and Wu, 1991; Orcutt *et al.,* 1993). We use a directional spectrum of the form proposed by Longuet-Higgins *et al.* (1963), $G(\theta) = L(q)\cos^q(\theta/2)$ where θ is the angle to the wind, q depends on frequency, and L is a normalization parameter. The functional form of q is not well determined (Massel, 1995) but is generally observed to vary from a value between about 5 and 10 (a very narrow directional spectrum) near the wave peak frequency to small values (a broad spectrum) at short periods. In constructing the curves shown in Figure 7, we assume q varies according to $q = 2 + 5/\{1 + \exp[5\log_{10}(fU/5)]\}$, where f is the wave frequency and U is the wind velocity. Comparisons between OBSs suggest that the absolute levels of each narrow-band-scatter plot shown in Figure 7 have an uncertainty of up to 6 dB. Given this data uncertainty, the fit of the model between 0.5 and 4 Hz (the frequencies at which noise is generated locally) is quite good.

It is important to realize that the model has significant limitations. The infinite ocean approximation ignores the interactions with the seabed and thus does not incorporate the resonant modes that will propagate in a finite-depth ocean. The model does not take into account the time for seas to develop or the tendency for the directional spectrum to broaden temporarily when winds shift (Webb and Cox, 1986). Perhaps most significantly, our functional form of $q(f)$, while plausible, has been chosen because it gives a good fit to the data. Despite these limitations, the model does illustrate some important features of all realistic microseism models. At a given frequency, there is a sharp wind-speed cutoff in microseism generation. For our model, this cutoff occurs at about 3 m/sec and 2 m/sec for 1-Hz and 4-Hz noise, respectively. At higher wind speeds where the wave amplitudes are saturated, a broadening directional spectrum produces noise levels that increase slowly with wind speed towards an asymptotic value. Clearly more data will be required before much confidence can be placed in a specific semiempirical relationship, but our results illustrate that this may be a promising approach to predicting seafloor noise.

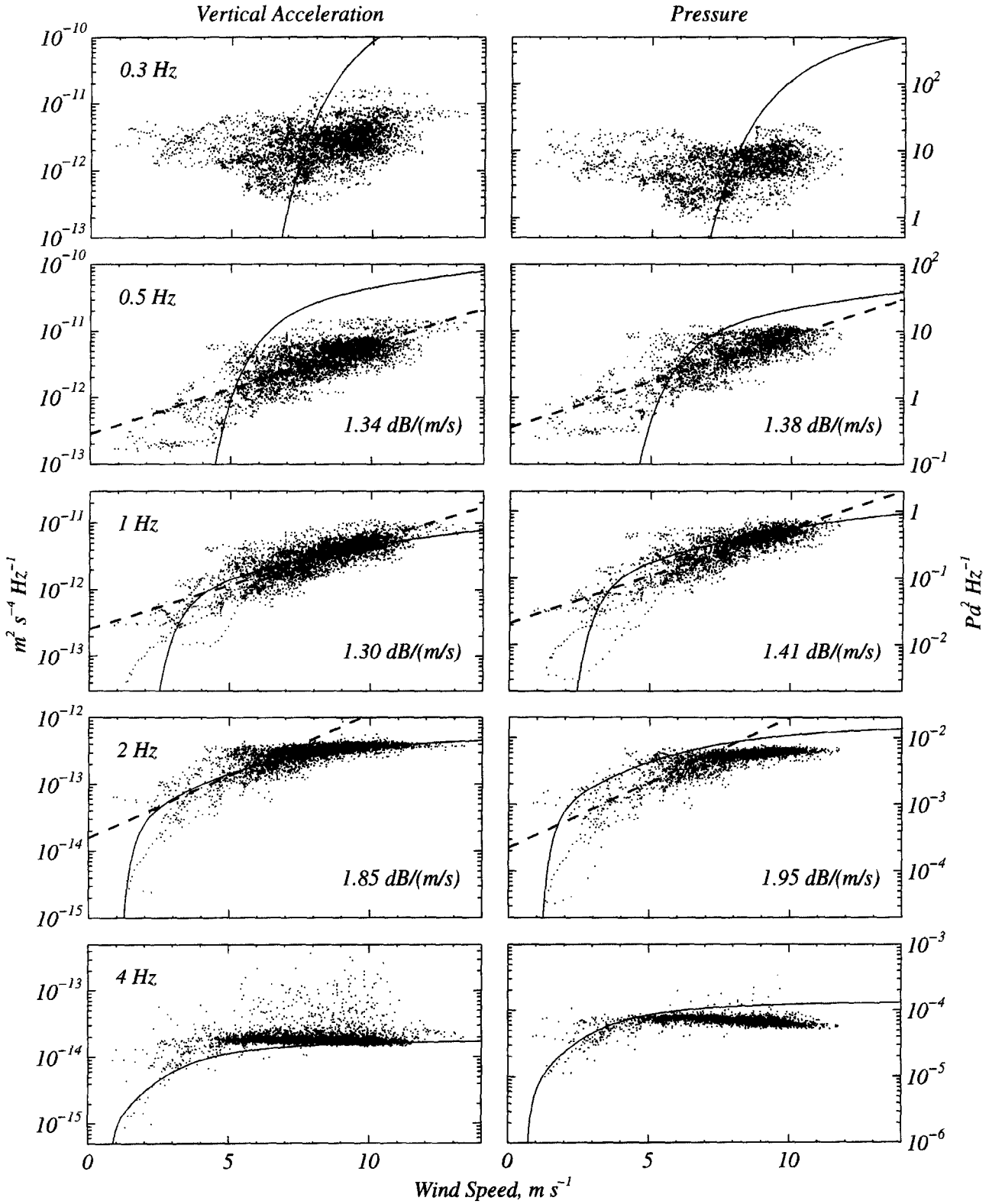

Figure 7. Scatter plots showing vertical acceleration and pressure noise levels at MELT site 3 as a function of wind speed for 0.3 octave bands centered at 0.3, 0.5, 1, 2, and 4 Hz. Least squared straight line fits (dashed) have been used to estimate the rate of increase of noise with wind speed at 0.5, 1, and 2 Hz. At 2 Hz the spectra clearly saturate so the fit is based on data for wind speeds below 7 m/sec. The solid lines show noise level predictions (see text) obtained for an infinite ocean model using the method of Webb (1992).

Iceland

Figure 8 shows time series of 6 months of noise and wind at ICEMELT station HOFF located near the southeast coast of Iceland. Wind data is shown for both the global data set (Atlas *et al.*, 1996) and a nearby meteorological station. Since SSM/I winds are not available over or near land, the global time series is essentially the ECMWF analysis. At all three frequencies shown, there are many features in common between the noise and wind time series. The average wind speed varies seasonally, and 1-Hz noise levels drop on average by about 5–10 dB during the summer. In general, the time series extracted from the global wind data set correlate slightly better than the local data. Since noise production is distributed over the sea surface, the spatial averaging inherent to the low-resolution global model is likely advantageous.

For all stations, the correlation coefficients between logarithmic noise and wind speed (Fig. 9) reach maximum values near 1 Hz but are slightly lower than observed at the MELT site (Fig. 6). At coastal station HOFF, the high correlation coefficients extend to noticeably higher frequencies than at station NYD, which is positioned 100-km inland. This observation is most easily explained if wind-generated ocean noise attenuates substantially as it moves inland. At frequencies below 0.3 Hz, seismic noise in Iceland is much better correlated with the local wind than at the MELT site. Cross correlation coefficients for the wind field near Iceland decrease below 0.5, when the two time series are separated by about 500 km. A significant portion of the noise near the microseismic peak must be produced locally. This is not surprising because Iceland is the site of many winter storms. Time lags between the noise and wind are relatively consistent between the two stations shown in Figure 9. They in-

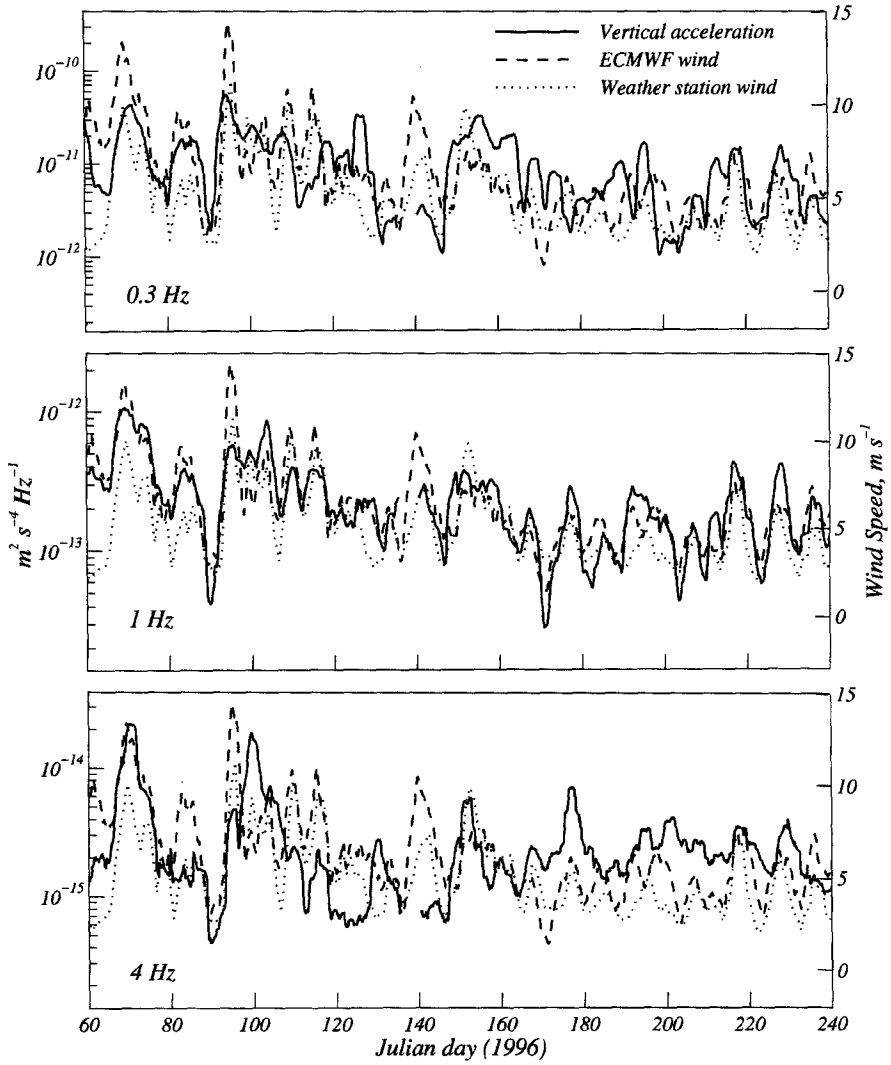

Figure 8. As for Figure 5, except the time series are for noise levels and wind at ICEMELT station HOFF. Wind speeds are shown for both the global dataset of Atlas *et al.* (1996) (dashed) and for a local weather station (dotted).

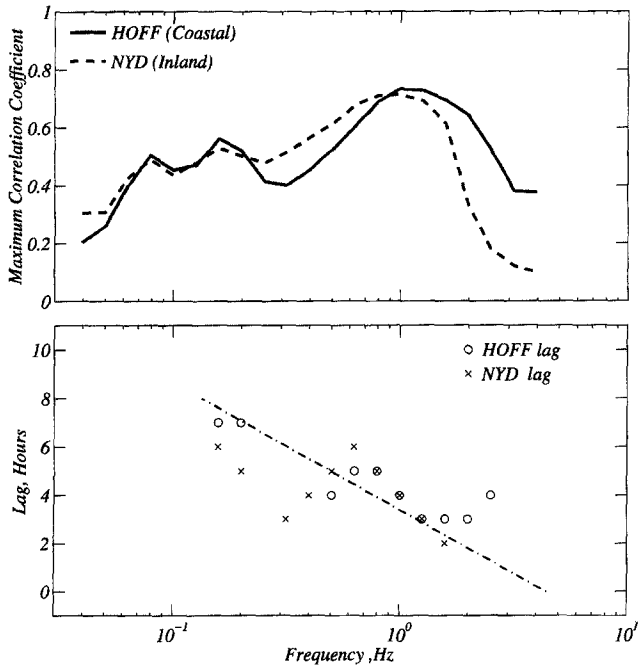

Figure 9. As for Figure 6 except the correlation coefficients and lags are for cross-correlations between wind speed (Atlas *et al.*, 1996) and the logarithm of vertical acceleration at ICEMELT station HOFF (solid lines and circles) and NYD (dashed line and crosses). The best fitting linear relationship between the lag, l (in hours) and the logarithm of frequency is $l = 3.3–5.3 \log_{10} f$.

crease noticeably more slowly with decreasing frequency than observed at the MELT site (Fig. 6) and show larger scatter.

At frequencies near 0.3 Hz, the average noise levels are fairly uniform and are not strongly dependent on the station location (Fig. 10). In contrast, there is a strong relationship between noise levels near 1 Hz and distance from the coast (Fig. 10). Stations that are about 100-km inland are about 10 dB quieter compared to stations within 20 km of the coast. If this is a result of attenuation of miscroseisms propagating inland as Rayleigh waves, then $Q_R \sim 100$. This value is reasonably consistent with values of apparent Q_s (100) and Q_P (60) estimated for the Icelandic upper crust (Menke *et al.*, 1995). Near 4 Hz, noise levels vary substantially between stations but are not strongly dependent on distance from the coast (Fig. 10). At such high frequencies, noise is not very strongly correlated with the wind speed (Fig. 9) and may reflect environmental conditions at the station site.

A comparison of scatter plots for logarithmic noise versus wind for ICEMELT (Fig. 11) and MELT (Fig. 7) shows that all the ICEMELT stations are consistently quieter at similar wind speed. For instance, at coastal station HOFF 1-Hz noise levels for wind speeds of 10 m/sec are about 10–15 dB lower than the MELT site. For a station on an infinite straight coastline, a difference of 6 dB would be expected because microseisms are not generated over land. Iceland is a small island, so this geometric effect should be smaller. In addition, absolute noise levels will change with differences in seismic impedance beneath station sites. Although the problem has not been studied in detail, it is likely that the acoustic modes which propagate short period microseisms in the oceans do not couple efficiently into land (Webb, 1998).

The scatter plots also reveal significant differences in the rate of increase of noise with wind. At the MELT site, noise at 0.5 and 1 Hz increases by about 1.3–1.4 dB per m/sec, and on Iceland the rate of increase averages 0.6–1 dB per m/sec. This difference cannot be due to simple attenuative affects, which would produce a constant offset to the scatter plots. It may reflect differences in the wave-directional spectrum. Alternatively, at low wind speeds, the background microseism level may be determined by energy that propagates from a broad source region as teleseismic body waves (Lacoss *et al.*, 1969).

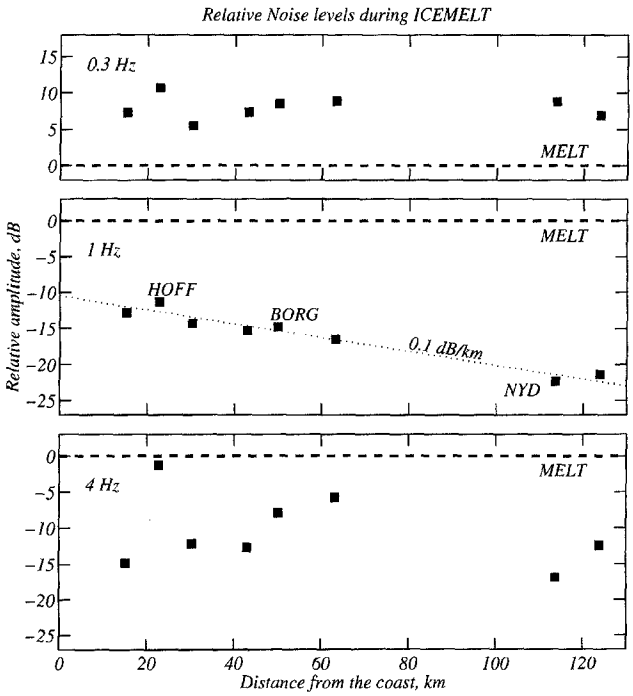

Figure 10. Vertical seismometer noise levels near 0.3, 1, and 4 Hz as a function of distance from the coast (open ocean) for seven ICEMELT stations and GSN station BORG (solid squares). For each ICEMELT station the relative noise level was obtained by calculating the average offset in decibels of hourly noise spectra relative to station BORG. The noise levels were averaged in 0.3 octave bands, and three–nine months of data was used at each station. These values were referenced to the noise levels at the MELT site (dashed lines) by comparing average noise levels recorded at MELT sites 3 and 5 with those recorded at BORG during 1996. At 1 Hz, the Iceland data is fit well by a slope of about 0.1 dB/km (dotted line).

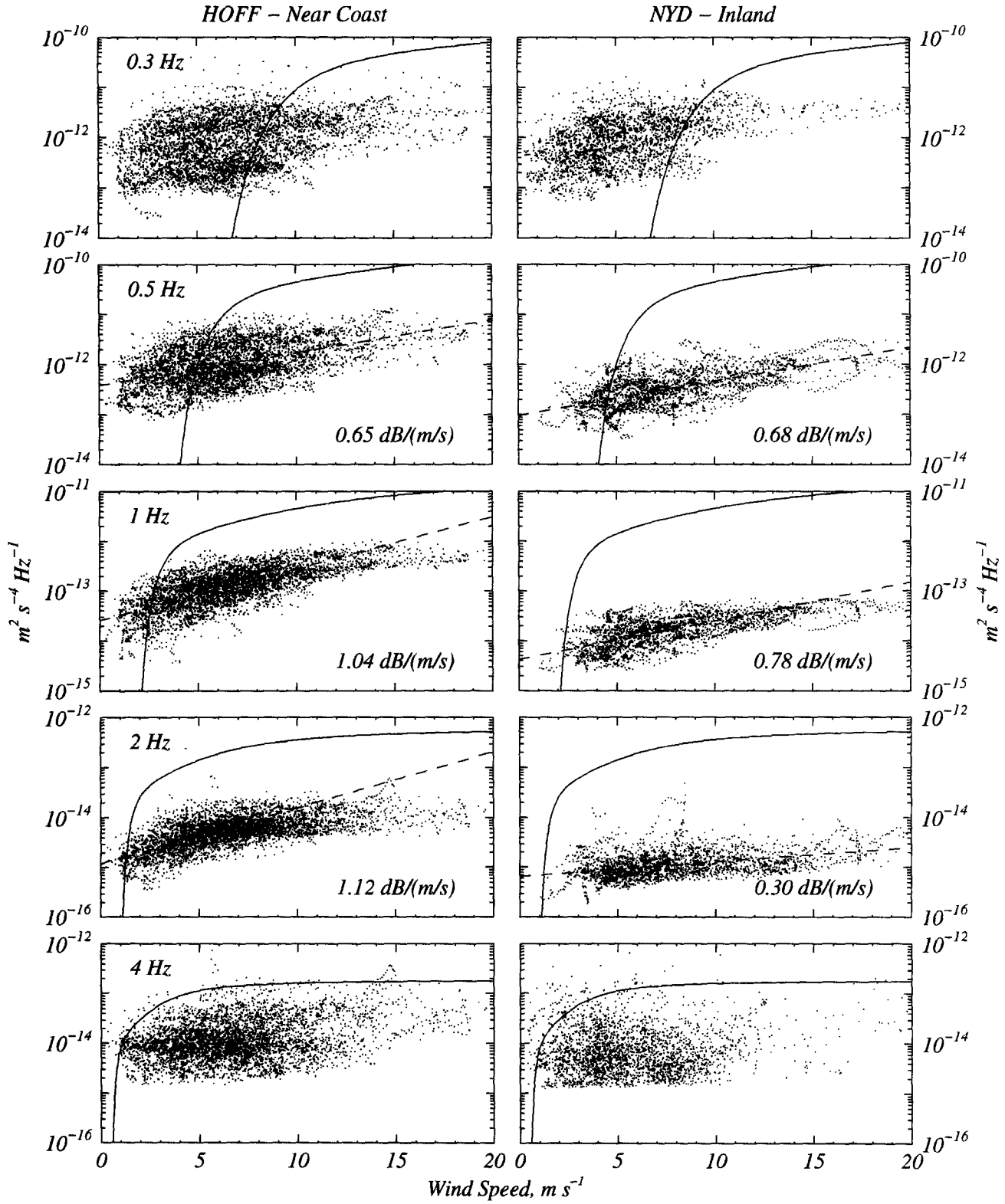

Figure 11. As for Figure 7, except scatter plots show vertical acceleration noise only for ICEMELT stations HOFF (left panel) and NYD (right panel).

Recording High-Frequency Teleseisms on Midocean Ridges using Teleseismic Arrivals

The problem of determining teleseismic detection limits for ocean floor experiments is addressed in some detail by Webb (1998). The amplitude of body waves from a particular event will be dependent on source characteristics and attenuation along the path. At any site, the expected frequency of occurrence of teleseisms exceeding an amplitude threshold will be dependent on both the distribution of sources and on the regional attenuation structure. Upper mantle attenuation is higher under oceans than continents and is probably highest along midocean ridges. Webb (1998) argues that the detection threshold for short period body waves may well exceed magnitude 7.5 at noisy ocean sites. The detection threshold for long period body waves is invariably much lower because of the lower noise levels below the microseism peak. The analysis also suggests that a 10 and 20 dB drop in noise levels will decrease the detection threshold for short period body waves by nearly 1 and 2 units of magnitude, respectively. Since there are only 2–3 earthquakes per year with $M \geqq 7.5$, but about 35 and 400 with $M \geqq 6.5$ and $M \geqq 5.5$, respectively, even short periods of quiet will greatly enhance the probability of a deployment recording high-frequency arrivals.

The noise data collected during the MELT experiment shows that noise levels near 1 Hz increase by about 1.3–1.4 dB per m/sec for winds above 5 m/sec and do not saturate until at least 10 m/sec. During the two exceptional intervals when smoothed winds dropped below 3–4 m/sec, noise on the vertical seismometers dropped by 15–20 dB to levels well below the predictions of linear regressions (Fig. 7). This observation is in reasonable agreement with a semiempirical wave model that predicts a sharp cutoff in 1-Hz noise at wind speeds below 3 m/sec (Fig. 7). Webb (1998) presents data for a 60-day deployment near 10°N on the EPR. Average SSM/I wind speeds during the experiment were about 5.5 m/sec (compared with 8.5 m/sec for MELT), and consequently the median noise levels were about 5 dB below the MELT experiment. Early in the 10°N deployment, the noise decreased by about 25 dB. This interval corresponds to a period when smoothed SSM/I derived winds dropped to about 2 m/sec, and the ship reported virtual calm. There were two other intervals later in the deployment when the smoothed wind speed dropped below 3 m/sec. During the first interval noise levels declined 15 dB. During the second the unsmoothed wind was temporally quite variable, and the noise levels decreased no more than 5–10 dB.

SSM/I wind speed data is not a perfect predictor of seismic noise near 1 Hz because the wind speeds have errors, and microseism generation is also dependent on the fetch, the duration, and changes in direction of the wind. However, on the basis of the limited data available, it seems that during intervals when the smoothed wind speed drops to 5 m/sec, 1 Hz noise levels are likely to fall ~7.5 dB below saturation levels. Intervals with smoothed wind speeds below 3 m/sec will usually coincide with noise drops of at least 15 dB. Webb (1998) shows that such decreases in noise should increase the probability of recording high-frequency body waves by factors of about 5 and 25, respectively.

Figure 12 summarizes the probability of encountering smoothed SSM/I derived wind speeds below 5 and 3 m/sec as a function of latitude along ridges in the Atlantic, Pacific, and Indian oceans. Significant maxima are labeled with the equivalent probability during the calmest three months of the year. In Figure 1, we highlight ridge sections where the sum of the probability of winds below 5 m/sec plus five times the probability of winds below 3 m/sec exceeds 0.4 (bold lines). On an annual basis, the calmest conditions are found along the northern EPR. The probability of wind speeds less than 3 m/sec increases from less than 0.05 near 10°N (the site of numerous seismic experiments) to over 0.25 at 16° N. In all three oceans, equatorial regions are calm (the doldrums). Equatorial wind speeds are noticeably higher on the mid-Atlantic ridge than in the Indian or Pacific, and the central Indian ridge is characterized by a particularly broad region of calm. During the calmest part of the year, the probability of low equatorial wind speeds is similar in all three ocean and is comparable to the northern EPR. On a three-month basis, the calmest conditions are found between February and April near 94° W on the Cocos-Nazca spreading center in the Pacific. Here the probabilities of wind speeds below 5 m/sec and 3 m/sec exceed 0.96 and 0.4, respectively, during February to April. There are two regions of significant calm at midlatitudes on the mid-Atlantic ridge, centered at 32° N and 22° S. Relatively calm conditions are also found on the southern EPR near 24° S. During the quietest three-month period, conditions at 24° S on the EPR are only slightly windier than similar latitudes on the mid-Atlantic ridge. It is also worth noting that the seafloor under the Arctic icecap is one of the quietest locations on the globe during the winter (Webb and Shultz, 1992) because the icecap prevents microseism generation.

Teleseismic high frequency body waves have only been recorded by OBSs deployed on midocean ridges in the Pacific for two very large earthquakes (Blackman *et al.*, 1995; Webb, 1998), and 0.5–1 Hz *P* waves have been observed for moderate sized events at three locations on ridges in the Atlantic and Indian Ocean (Fig. 1) (Rowlett and Forsyth, 1979; Blackman *et al.*, 1995; Forsyth, 1996; Sato *et al.*, 1996). It is clear from Figure 12 that there are ridge sections in the Pacific that are as calm as the quietest sites in other oceans, but to date deployments have not generally been located in these calm areas. It is also worth noting that although the MELT experiment was characterized by a reasonable distribution of sources (Forsyth *et al.*, 1998), the weather was relatively poor. Periods of near calm are rare in the southern Pacific, but the probability of smoothed wind speeds below 5 m/sec near 17° S is about 17%. During the MELT deployment, the trades were particularly consistent, and smoothed wind speeds dropped below 5 m/sec for only 7% of the experiment.

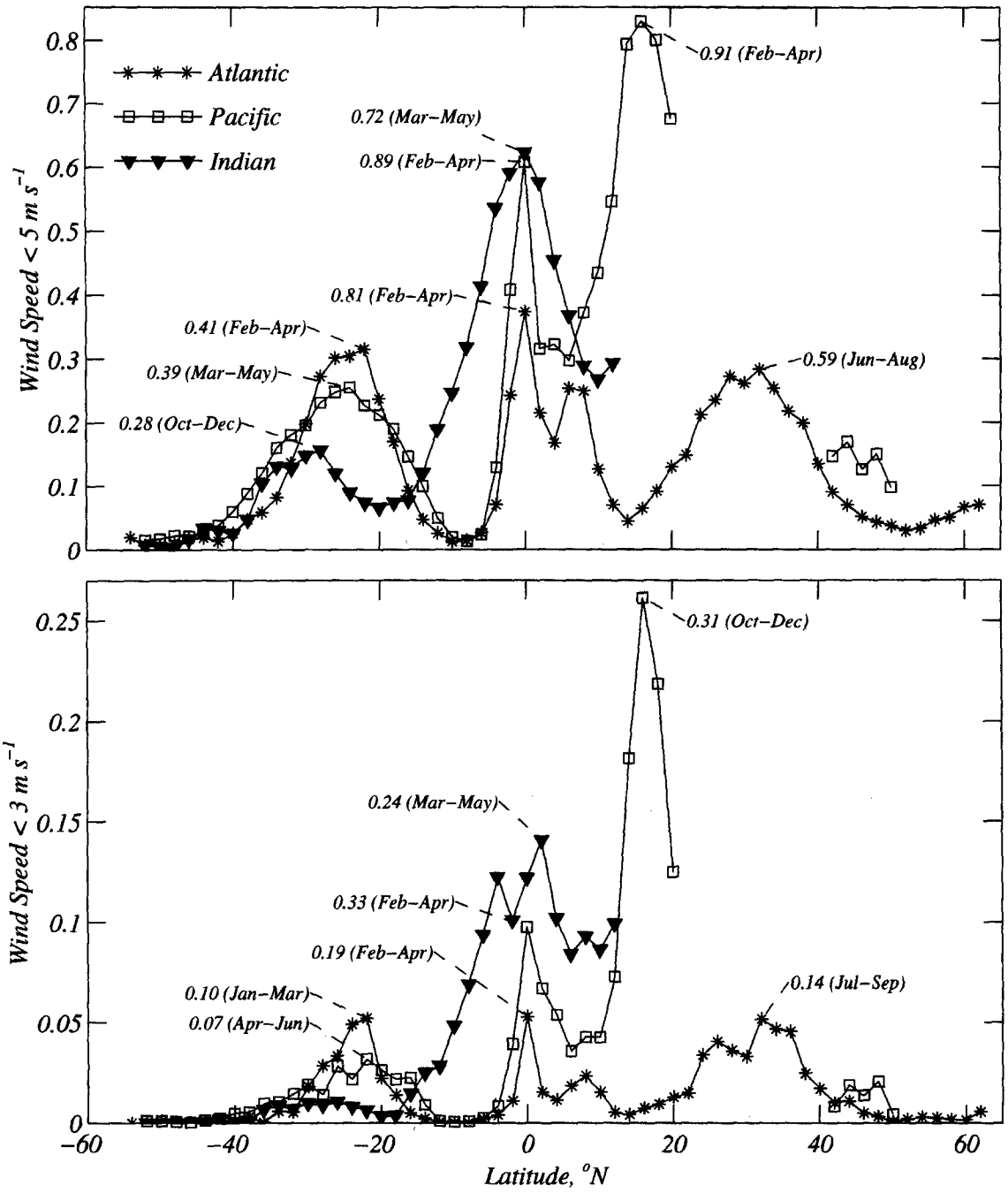

Figure 12. Proportion of time the smoothed SSM/I derived wind speed (Atlas *et al.*, 1996) drops below 5 m/sec (top) and 3 m/sec (bottom) as a function of latitude along midocean ridges in the Atlantic (asterisks), Pacific (open squares), and Indian oceans (solid triangles). Labels show the equivalent values derived from data for the calmest 3 months of the year. The plot is derived from 5 years of wind data between 1992 and 1996, smoothed with a 3-day running mean. In the Pacific ocean, data is shown for the Juan de Fuca Ridge, the east Pacific rise, and the Pacific-Antarctic Ridge north of 52° S. In the Indian ocean the data is for the central Indian ridge and the southeast Indian ridge north of 52° S. For ridges in the southern ocean that are not shown in this plot, the probabilities of winds below 5 m/sec and 3 m/sec are always less than 0.1 and 0.02, respectively, except for the southwest Indian ridge near the Rodriguez triple junction. On the Cocos(Galapagos)–Nazca spreading center, the probabilities of smoothed winds below 5 m/sec and 3 m/sec are about 0.4 and 0.1, respectively.

Of the three experiments that reported high-frequency arrivals in the Atlantic and Indian Oceans, only the deployment near 35° N on the MAR is located in a calm region (Fig. 1). Forsyth (1996) reports calm conditions for this experiment, which occurred in June 1980. The other two deployments were located at sites where the average winds are substantially higher than the MELT site (Fig. 12). At 11° N on the MAR, Rowlett and Forsyth (1979) recorded a single intermediate depth earthquake from Southern Peru in December, 1977. At this time of year, the probability of smoothed wind speeds less than 5 m/sec is only 1%. Six earthquakes with magnitudes ranging from 5.8 to 7.2, and epicentral distances between 62 and 82° were recorded with reasonable signal-to-noise ratios at 0.5–1 Hz in August, 1993 on the Rodriguez triple junction. Both the cruise report (Tamaki and Fujimoto, 1995) and the SSM/I derived winds suggest that wind speeds were 6–8 m/s.

There are presently insufficient observations to determine whether the threshold for recording high-frequency body waves at a given local wind speed varies between midocean ridges. The existing data does not exclude the possibility that the detection thresholds may be higher on the EPR for a given wind speed. Webb and Cox (1986) show that peak microseismic noise levels can vary between ocean basins, because the microseisms attenuate more rapidly in ocean basins with thick sediment layers. Midocean ridges are generally unsedimented and since microseismic noise near 1 Hz is generated locally, it is unlikely that basin scale variations in sedimentation can account for variations in high-frequency detection thresholds. There are numerous studies which show that mantle attenuation is generally high beneath the Pacific and in particular beneath the EPR (Bussy *et al.*, 1993; Canas and Mitchell, 1978; Ding and Grand, 1993). Further deployments will be required to determine whether body waves recorded on the East Pacific Rise are more attenuated than on other ridges.

Conclusions

In this article, we have compared noise levels recorded during the MELT and ICEMELT experiments. The large difference in signal-to-noise ratios for high-frequency body waves is at least in part a consequence of 1-Hz noise levels that are 10–20 dB higher at the MELT site. At both sites, noise at 0.5–2 Hz is well correlated with wind speeds obtained from a global data set that incorporates satellite data. The lower noise levels on Iceland suggest that 1-Hz microseisms couple poorly into continents and a comparison of noise levels with distance from the coast shows that the microseisms attenuate as they travel inland. This study both confirms earlier work which showed that high-frequency microseismic noise is generated locally by waves (Webb, 1998) and demonstrates the predictive powers of satellite wind measurements. Global data sets of satellite derived wind speeds should be used to select the quietest sites for future teleseismic experiments on midocean ridges and for seafloor stations in the permanent global seismic network.

Acknowledgments

We thank W. C. Crawford and C. E. Golden for help at sea during the MELT experiment and Tom Deaton and Jacques Lemire, who are the lead engineers on the OBSs. We are grateful to the many Icelandic farmers for their generous assistance with the ICEMELT experiment, the staff of the National Electric Company of Iceland (Landsvirkjun), A. Kuehnel, R. Kuehnel, H. Brynjólfsson, and the staff of the PASSCAL Instrument Pool. We thank Charles McCreery and John Orcutt for thorough reviews of an earlier draft. This study was supported by the National Science Foundation under grant OCE-9414299.

References

Adair, R. G., J. A. Orcutt, and T. H. Jordan (1984). Analysis of ambient seismic noise recorded by downhole and ocean-bottom seismometers on deep sea drilling project leg 78B, *Initial Rep. Deep Sea Drill. Proj.* **78,** 767–780.

Atlas, R., R. N. Hoffman, S. C. Bloom, J. C. Jusem, and J. Ardizzone (1996). A multilayer global surface wind velocity dataset using SSM/I wind observations, *Bull. Am. Meteor. Soc.* **77,** 869–882.

Babcock, J. M., B. A. Kirkendall, and J. A. Orcutt (1994). Relationships between ocean bottom noise and the environment, *Bull. Seism. Soc. Am.* **84,** 1991–2007.

Bjarnason, I. T., C. J. Wolfe, S. C. Solomon, and G. Gudmundson (1996). Initial results from the ICEMELT experiment: Body-wave delay times and shear-wave splitting across Iceland, *Geophys. Res. Lett.* **23,** 459–462.

Blackman, D. K., J. A. Orcutt, and D. W. Forsyth (1995). Recording teleseismic earthquakes using ocean-bottom seismographs at mid-ocean ridges, *Bull. Seism. Soc. Am.* **85,** 1648–1664.

Bromirski, P. D., and F. K. Duennebier (1998). Swell-induced near coastal microseisms (abstract), *Eos Trans. AGU* **79,** Fall Meeting Suppl., F662.

Bussy, M., J. P. Montagner, and B. Romanowicz (1993). Tomographic study of upper mantle attenuation in the Pacific Ocean, *Geophys. Res. Lett.* **20,** 663–666.

Canas, J. A., and B. J. Mitchell (1978). Lateral variation of surface-wave anelastic attenuation across the Pacific, *Bull. Seism. Soc. Am.* **68,** 1637–1640.

Coffin, M. F., L. M. Gahagan, and L. A. Lawver, (1998). Present-day plate boundary digital data compilation, *Technical Report No. 174,* University of Texas Institute for Geophysics, Austin, Texas.

Cox, C. S., T. Deaton, and S. C. Webb (1984). A deep sea differential pressure gauge, *J. Atmos. Oceanic Technol.* **1,** 237–246, 1984.

Crawford, W., S. Webb, and J. Hildebrand (1993). Shear velocity structure on the Juan de Fuca ridge from seafloor compliance measurements (abstract), *EOS Trans. AGU* **74,** Fall Meeting Suppl., 604.

Ding, X.-Y., and S. P. Grand (1993). Upper mantle Q structure beneath the East Pacific Rise, *J. Geophys. Res.* **98,** 1973–1985.

Dorman, L. R., A. E. Schreiner, L. D. Bibee, and J. A. Hildebrand (1993). Deep-water sea-floor array observations of seismo-acoustic noise in the eastern Pacific and comparisons with wind and swell, in *Natural Physical Sources of Underwater Sound,* B. R. Kerman (Editor), Kluwer Academic, Boston, 165–174.

Forsyth, D. W. (1996). Partial melting beneath a Mid-Atlantic Ridge segment detected by teleseismic PKP delays, *Geophys. Res. Lett.* **23,** 463–466.

Forsyth, D. W., D. S. Scheirer, S. C. Webb, L. M. Dorman, J. A. Orcutt, A. J. Harding, D. K. Blackman, J. Phipps Morgan, R. S. Detrick, Y. Shen, C. J. Wolfe, J. P. Canales, D. R. Toomey, A. F. Sheehan, S. C. Solomon, and W. S. D. Wilcock (1998). Imaging the deep seismic structure beneath a midocean ridge: The MELT experiment, *Science* **280,** 1215–1218.

Hasselmann, K. A. (1963). A statistical analysis of the generation of microseisms, *Rev. Geophys. Space Phys.* **1,** 177–210.

Hollinger, J., R. Lo, G. Poe, R. Savage, and J. Pierce, (1987). Special Sensor Microwave/Imager user's guide, *Technical Report,* Navy Research Laboratory, Washington, D. C.

Kibblewhite, A. C., and C. Y. Wu (1991). The theoretical description of wave-wave interactions as a noise source in the ocean, *J. Acoust. Soc.* **89,** 2241–2252.

Kibblewhite, A. C., and C. Y. Wu (1996). *Wave Interactions as a Seismo-acoustic Source,* Springer, New York, 313 pp.

Lacoss, R. T., E. J. Kelly, and M. N. Toksöz (1969). Estimation of seismic noise structure using arrays, *Geophysics* **34,** 21–38.

Levchenko, D. G., S. L. Soloviev, A. V. Son'kin, and E. V. Voronina (1994). Recording of ocean-bottom seismic noise and of a strong earthquake in the Himalayas by broadband digital OBS installed on the Mid-Atlantic Ridge, *Phys. Earth Planet. Inter.* **84,** 305–320.

Lewis, B. T. R., and L. R. Dorman (1992). Recording teleseisms on the seafloor; an example from the Juan de Fuca plate (abstract), *EOS Trans. AGU* **73,** 202.

Longuet-Higgins, M. S., D. E. Cartwright, and N. D. Smith (1963). Observations of the directional spectrum of sea waves using motions of a floating buoy, in *Ocean Wave Spectra,* Prentice Hall, Englewood Cliffs, New Jersey, 111–136.

Massel, S. R. (1995). *Ocean Surface Waves: Their Physics and Prediction,* World Scientific, New Jersey, 491 pp.

McCreery, C. S., F. K. Duennebier, and G. H. Sutton (1993). Correlation of deep ocean noise (0.4–30 Hz) with wind, and the Holu spectrum—A worldwide constant, *J. Acoust. Soc.* **93,** 2639–2648.

Menke, W., V. Levin, and R. Sethi (1995). Seismic attenuation in the crust at the mid-Atlantic plate boundary in south-west Iceland, *Geophys. J. Int.* **122,** 175–182.

Montagner, J.-P., J.-F. Karczewski, B. Romanowicz, S. Bouaricha, P. Logonné, G. Roult, E. Stutzmann, J.-L. Thirot, J. Brion, B. Dole, D. Fouassier, J.-C. Koenig, J. Savary, L. Floury, J. Dupond, A. Echardour, and H. Floc'h (1994). The French pilot experiment OFM-SISMOBS: first scientific results on noise level and event detection, *Phys. Earth. Planet. Inter.* **84,** 321–336.

Orcutt, J. A., C. S. Cox, A. C. Kibblewhite, W. A. Kuperman, and H. Schmidt (1993). Observations and causes of ocean and seafloor noise at ultra-low and very-low frequencies, in *Natural Physical Sources of Underwater Sound,* B. R. Kerman (Editor), Kluwer Academic, Boston, 203–232.

Orcutt, J. A., and G. M. Purdy (1995). *Broadband Seismology in the Oceans—Towards a Five-Year Plan,* Joint Oceanographic Institutions Inc., Washington, DC, 105 pp.

Pierson, W. J., and L. Moskowitz (1964). A proposed spectral form for fully developed wind seas based on the similarity theory of S. A. Kiaigorodskii, *J. Geophys. Res.* **69,** 5181–5190.

Purdy, G. M., and A. D. Dziewonski (1988). *Proceedings of a Workshop on Broad Band Seismometers in the Deep Ocean,* Woods Hole Oceanographic Institution, Woods Hole, Mass., 331 pp.

Rowlett, H., and D. Forsyth (1979). Teleseismic *P*-wave delay times in a major oceanic fracture zone, *Geophys. Res. Lett.* **6,** 273–276.

Sato, T., K. Katsumata, J. Kasahara, N. Hirata, R. Hino, N. Takahashi, M. Sekine, S. Miura, and S. Koresawa (1996). Travel-time residuals of teleseismic *P*-waves at the Rodriguez triple junction in the Indian Ocean using ocean-bottom seismometers, *Geophys. Res. Lett.* **23,** 713–716.

Tamaki, K., and H. Fujimoto, (1995). R/V Hakuho-maru KH93-3 Research Cruise July 8–September 17, 1993. Preliminary Cruise Report, Ocean Research Institute, University of Tokyo, Tokyo, Japan.

Toomey, D. R., W. S. D. Wilcock, S. C. Solomon, W. C. Hammond, and J. A. Orcutt (1998). Mantle seismic structure beneath the MELT region of the East Pacific Rise from *P* and *S* wave tomography, *Science* **280,** 1224–1227.

Trenberth, K. E., (1992). Global analyses from ECMWF and Atlas of 1000 to 10 mb Circulation Statistics. Tech. Rep. NCAR/TN-373 + STR, National Center for Atmospheric Research, Boulder, Colorado.

Webb, S. C. (1992). The equilibrium oceanic microseism spectrum, *J. Acoust. Soc. Am.* **92,** 2141–2158.

Webb, S. C. (1998). Broadband seismology and noise under the ocean. *Rev. Geophys.* **36,** 105–142.

Webb, S. C., and C. S. Cox (1986). Observations and modeling of seafloor microseisms, *J. Geophys. Res.* **91,** 7343–7358.

Webb, S. C., and A. D. Shultz (1992). Very low frequency ambient noise at the seafloor under the Beaufort Sea icecap, *J. Acoust. Soc. Am.* **91,** 1429–1439.

Webb, S. C., X. Zhang, and W. Crawford (1991). Infragravity waves in the deep ocean, *J. Geophys. Res.* **96,** 2723–2736.

Wentz, F. J. (1997). A well-calibrated ocean algorithm for special sensor microwave/imager, *J. Geophys. Res.* **102,** 8703–8718.

Wolfe, C. J., I. T. Bjarnason, J. C. VanDecar, and S. C. Solomon (1997). Seismic structure of the Iceland mantle plume, *Nature* **385,** 245–247.

School of Oceanography
University of Washington
Box 357940
Seattle, WA 98195
(W.S.D.W)

Marine Physics Laboratory, 0205
Scripps Institution of Oceanography
University of California
LaJolla, CA 92093
(S.C.W.)

Science Institute
University of Iceland
Reykjavík, Iceland
(I.Th.B)

Manuscript received 4 January 1999.